JOURNAL OF AIRCRAFT
Vol. 45, No. 5, September–October 2008

Adaptive Eulerian Modeling for Air Traffic Flow Management

Aditya P. Saraf* and Gary L. Slater†
University of Cincinnati, Cincinnati, Ohio 45221

DOI: 10.2514/1.32870

A method for deriving an Eulerian traffic flow model in real time without depending on online integration of aircraft trajectories is introduced. In this method, online model derivation starts with a baseline Eulerian airspace model, which is derived offline using historical track data. In real time, parameters of this baseline model are adapted depending on the differences in flight plans and control volume aircraft counts between the baseline model and the real world. The baseline model derivation method is based on bookkeeping of control volume aircraft counts and, hence, the model produces control decisions in terms of whole number aircraft counts, unlike the fractional counts produced by Eulerian models based on average aircraft speeds. The bookkeeping-based model indirectly retains trajectory information and aircraft identities. Hence, it serves as an excellent tradeoff between Eulerian and trajectory-based modeling approaches. Most importantly, as an improvement over previous approaches, we take into consideration the control-dependent nature of the Eulerian model while computing optimal flow-control decisions. A key feature of this model is the use of interstream jump (γ) parameters. These parameters make the model easily amenable to emulate a wide variety of control actions like rerouting. As a proof of concept, we derive a baseline model for the Fort Worth center from recorded track data for a period of 1 h on 13 March 2005 and adapt it to predict sector counts for another time period. An application of the adaptive model to optimal rerouting is also presented.

I. Introduction

ACCORDING to the International Air Transport Association's (IATA) 2006 Annual Report [1], despite the ill effects of September 2001 events, the airline industry is slowly returning to normalcy. The increase in traffic volumes during the year 2005 bears out this fact. In that year, freight traffic volume increased by 5%, and airline revenues increased by 9%. Air traffic went up by 7% in 2005 [2]. Also, since the slump in passenger traffic during the recession of 2001–2003, the number of airline passengers has risen by almost a quarter, to over two billion. It is estimated that this trend will continue, with the world passenger traffic growing at an annual rate of 4.8% and freight traffic growing at an annual rate of 6% [2] over the period 2006–2025. Similar trends have been predicted for the air traffic in the United States. This increase in demand will put further stress on the already fully used resources of the U.S. National Airspace System (NAS), especially busy enroute sectors and Terminal Radar Approach Control (TRACON) regions around busy airports. Hence, recently there has been a lot of interest in the air traffic management community toward new air traffic flow management concepts with emphasis on the issue of congestion problems. The broad aim of these research initiatives is to find efficient ways to prevent the density of aircraft from becoming too large in any region of the airspace while seeking to maximize the throughput at all the airports in the region.

At present, methods for air traffic flow prediction in air traffic management (ATM) compute future aircraft counts by propagating aircraft trajectories of proposed flights forward in time, using the current state of the system, filed flight plans, aircraft type dependent aeropropulsive models, and standard ascent/descent profiles. The Center TRACON Automation System (CTAS) [3] and future ATM Concepts Evaluation Tool (FACET) [4] use such a trajectory-based approach for traffic flow prediction. The accuracy of these predictions is highly influenced by uncertainties in weather and departure times, and they depict the behavior of the NAS with adequate accuracy for up to 20 min in the future [5]. Such a short prediction horizon, however, is not enough for making sound strategic flow management decisions.

Low-dimensional airspace models [6–10], which are based on aggregate flow properties of the aircraft flows, have been found to be more useful in air traffic flow management. Such models, called Eulerian models, divide the airspace into control volumes and model the traffic flow in the airspace in terms of conservation equations. In past approaches, the derivation of Eulerian models in real time depended on fast online integration of aircraft trajectories using the available position, velocity, and flight plan information. For a large airspace such as the NAS, online integration of aircraft trajectories for all the aircraft involved signifies a large computational burden, especially when the prediction horizon is long. Uncertainties in long-term trajectory predictions also render such models, derived from online trajectory integrations, inaccurate.

The purpose of this paper is to devise a method for real-time derivation of Eulerian models without depending on online trajectory integrations. This method starts with a baseline Eulerian model of the airspace. This model is derived offline using recorded track data. In real time, differences in control volume aircraft counts and flight plans between the baseline model predictions and the real-world measurements are used to adapt the baseline model to match the real world. The adapted model can then be used in a simulation-based optimization scheme to achieve optimal traffic flow management. Figure 1 explains the model adaptation process pictorially. In the next paragraph, we review the basic principles behind Eulerian models and recap some technical contributions, which illustrate the potential for the use of such models in air traffic management.

In the Eulerian modeling approach, the airspace is divided into control volumes, and aircraft in each control volume are treated as a single unit based upon their aggregate flow properties. Menon et al. [7–10] present a spatially discretized approach toward traffic flow management (TFM). They divide the airspace into control volumes and use the physical dimensions of each control volume and the average velocity of aircraft within each control volume to generate an Eulerian model of air traffic flow as a network of interconnected

Presented as Paper 7857 at the 7th AIAA Aviation Technology, Integration, and Operations (ATIO), Belfast, Northern Ireland., 18–20 September 2007; received 17 June 2007; revision received 6 February 2008; accepted for publication 7 February 2008.

*Graduate Research Assistant, Department of Aerospace Engineering and Engineering Mechanics. Student Member AIAA.

†Professor Emeritus, Department of Aerospace Engineering and Engineering Mechanics. Associate Fellow AIAA.

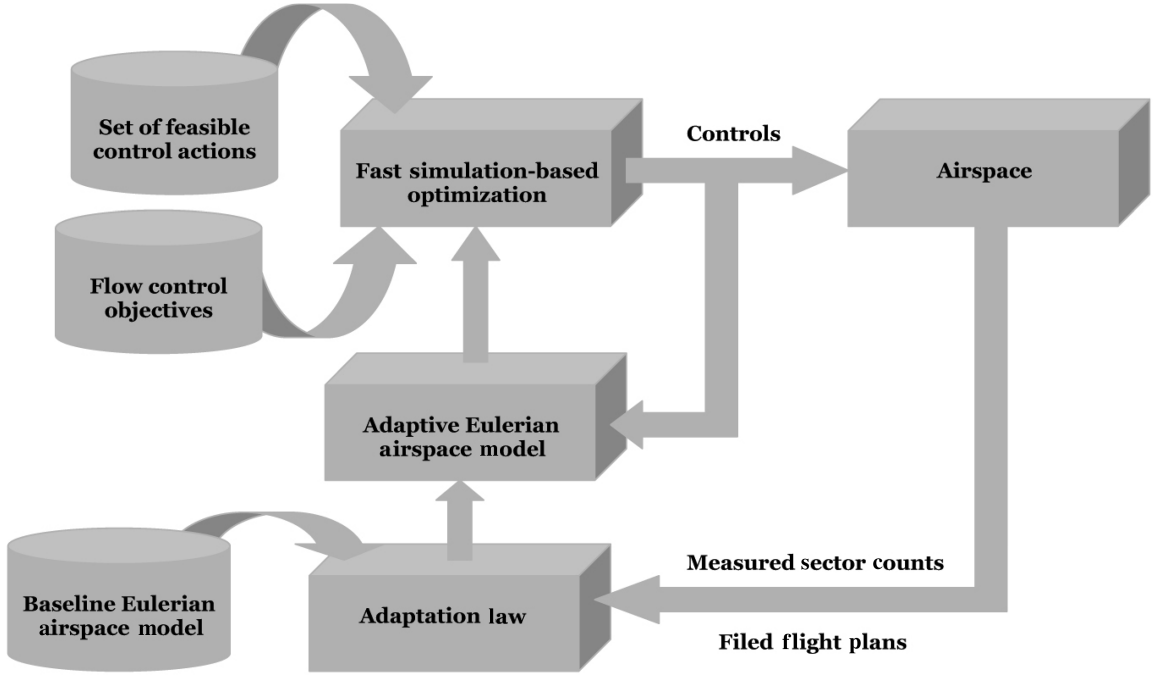

Fig. 1 Simulation-based optimization process.

control volumes. The rationale behind using Eulerian models of the airspace as opposed to trajectory-based (Lagrangian) models is that the low-dimensional Eulerian models are easier to iterate forward in time to obtain future sector count predictions. Dynamic representation of each aircraft requires at least three differential equations, and so the order of a trajectory-based model goes up linearly with the number of aircraft. On the other hand, in the case of Eulerian models, the model order depends only on the number of control volumes and not on the total number of aircraft in the airspace. In fact, the accuracy of Eulerian models goes up with the number of aircraft, because as the density of aircraft increases, the traffic flow more accurately mimics continuous flows like the ones encountered in fluid mechanics or heat transfer. Some other references that deal with the use of Eulerian models in ATM are Bayen et al. [11,12] and Sridhar [5]. In our approach, we have used a spatially discretized model similar to that of Menon et al. for modeling the airspace.

Although our works builds on previous research work in the area of Eulerian modeling, there are some key differences between our approach to Eulerian model derivation and the previous approaches. The most important difference is that we do not rely on real-time trajectory integrations for updating our model. Instead, we adapt the model online based on differences between the real world and the model. Furthermore, because we derive the baseline model offline and already have full predicted trajectories for all the aircraft, we do not rely on average aircraft velocities for deriving the model. Instead, we directly derive the model parameters by looking at numbers of aircraft transitioning from one control volume to the other in each discrete time step. This bookkeeping-based model-derivation process is explained in detail in Sec. II.B. Eulerian model control decisions are in the form of hold backs or slow downs applied to a whole group of aircraft. A nonzero control input inherently modifies the Eulerian model. Most previous works related to the use of Eulerian models in ATM do not consider this control dependence. In our work, we build on these previous works, especially Menon et al. [7–10], which are seminal works in the area of the use of Eulerian models in ATM, and we take a further step by acknowledging the control-dependent nature of the Eulerian model while formulating the optimal TFM problem as a model-based optimization problem. To this end, in our model-based optimization scheme, we make necessary adaptations to the model at each time step when the control inputs are nonzero. Finally, models based on average aircraft velocities do not preserve individual aircraft identity or trajectory information, which makes it difficult to map control decisions back to individual aircraft. In the bookkeeping-based model, trajectory information is indirectly retained in the sense that each aircraft's path as it moves from one control volume to the other can be tracked by looking at the model parameters.

A key feature of this model, which enables retention of trajectory information in the face of traffic flow control actions, is the use of interstream jump (γ) parameters. These parameters enable the model to be adapted to simulate the effects of a wide variety of air traffic control (ATC) actions like rerouting, speed reductions, sector closures, etc. All we need to do to modify an aircraft's path is to change the model parameters in such a way that an aircraft following the old track is removed, and an aircraft following the new track is added to the model (more on this in Sec. III). Because of all these features, this adaptive model is of very high utility in air traffic management in the sense that it can be used to simulate the effects of different candidate ATC actions quickly and then the best one can be chosen based on the model predictions.

As a proof of concept, we derive a baseline model for the Fort Worth center using an hour-long recorded air traffic data on 13 March 2005. We then adapt the baseline model to predict sector counts for another time period. We also demonstrate the use of the Fort Worth center adaptive Eulerian model in a simulation-based optimization scheme for making optimal rerouting decisions. The paper is organized as follows: Sec. II explains the derivation of the baseline Eulerian model from recorded air traffic data. The Fort Worth center is chosen as the airspace to model. Section III gives a detailed description of the process by which the baseline model is adapted to match the real-world situation. This section also presents the validation of this adapted model against real observed traffic. Section IV.B presents an example that displays the versatility of the adaptive aggregate model in simulating the effects of one of the most complex ATC actions: optimal rerouting of aircraft around a closed airspace. Finally, Sec. V presents some conclusions and discusses directions for further research.

II. Derivation of the Baseline Eulerian Model from Recorded Air Traffic Data

In this section, we present a bookkeeping-based Eulerian model-derivation process. In particular, we describe the derivation of a

baseline Eulerian model for the Fort Worth center (ZFW) airspace using recorded Enhanced Traffic Management System (ETMS) data.

A. Bookkeeping-Based Eulerian Airspace Model

The baseline model-derivation process begins by dividing the modeled airspace into control volumes. The traffic flow is modeled by equations for conservation of aircraft for each control volume. We will explain the bookkeeping-based model with an example of Eulerian model derivation for the Fort Worth center. For modeling purposes, the ZFW center was divided into 12 control volumes, each control volume consisting of one or more high-level and low-level sectors. We chose to group sectors together into 12 control volumes to achieve a compromise between a highly detailed, high-computational-burden model at one end and a low-order, low-fidelity model on the other. Low-level sectors were coupled together with one or more high-level sectors to keep track of aircraft at all altitudes while refraining from creating separate control volumes for each individual sector, thus keeping the order of the model low. Figure 2 shows the high-level ZFW sectors and the location of the Dallas–Fort Worth Airport (DFW). The modeled region consists of all ZFW sectors. The Albuquerque center (ZAB), the Memphis center (ZME), the Kansas City center (ZKC), and the Houston center (ZHU) surround the modeled region. Control volumes adjacent to these unmodeled regions get inflows from the neighboring unmodeled regions, and some aircraft from these control volumes go out to the unmodeled regions. Table 1 lists the low-level and high-level sectors associated with each of the 12 control volumes. For example, the first control volume is made up of the high-level sector ZFW46 and a number of low-level sectors lying below the ZFW46 airspace. The high sectors in ZFW center adjacent to this control volume are ZFW48, ZFW90, ZFW71, ZFW89, ZFW65, ZFW39, ZFW94, and ZFW47. There are two external sectors (external to the modeled airspace) adjacent to this sector: ZHU82 and ZHU78. ZFW46 will get inflows from all these adjacent sectors. Similarly, the other control volumes are groupings of one or more high-level and low-level sectors.

As we see from Fig. 2, each control volume is surrounded by multiple control volumes and gets inflows from some or all of them. Because of such nature of the airspace, we divide the aircraft flows in each control volume into multiple streams; each stream of aircraft is associated with one of the adjacent control volumes. For example, there are eight control volumes surrounding the ZFW46 control volume; these are the control volumes associated with the sectors ZFW48, ZFW90, ZFW71, ZFW89, ZFW65, ZFW39, ZFW94, and ZFW47, respectively. The aircraft flows in the ZFW46 control volume are divided into eight streams, each stream containing aircraft going out to one of the adjacent control volumes. The ZFW46's control volume is also bordered on the south by some Houston center sectors. So, it has a ninth stream, consisting of aircraft going out to the Houston center. Finally, there are multiple airports within ZFW46, and so there will be an additional tenth stream associated with the aircraft that land at these airports. If a particular control volume contains multiple airports, then it is even possible to assign separate streams for each airport. Table 1 shows the streams associated with each control volume for the airspace under consideration.

In the baseline model-derivation process, each aircraft present in a control volume will be allocated to one of the streams in the control volume, depending on the adjacent control volume that it will enter. (Note that the baseline model is derived from recorded track data, and so information regarding which control volume the aircraft will enter next is available from the aircraft's stored trajectory.) For example, an aircraft taking off at the Dallas–Fort Worth airport and heading for the Houston airport will normally transit from sector ZFW46 to the Houston center. Houston center is associated with the ninth stream for this control volume (refer to Table 1). Hence, this aircraft will be assigned to the ninth stream within ZFW46's control volume.

The aircraft count in each stream is a component of the state vector of the Eulerian model. Time is discretized for modeling purpose. At each time step, we derive a linear relationship between stream aircraft counts at the previous and the current time steps, for each of the streams. This gives a discrete time, linear, time-varying Eulerian model. There are a number of modeling parameters associated with each stream. The $\alpha^{(i,i)}(k)$ parameter gives the ratio of aircraft that remain back in the ith stream after the passage of one discrete time interval from the kth to the $(k+1)$th time step to the number of aircraft present in the ith stream at the kth time step. The $\beta^{(i,j)}(k)$ parameter gives the ratio of the number of aircraft coming in through the jth stream and going out into the ith stream during the time interval from the kth to the $(k+1)$th time step to the total number of aircraft coming in through the jth stream during the same time period. The $\gamma^{(i,j)}(k)$ parameter gives the ratio of the number of aircraft present in the jth stream at the kth time step that change over to the ith stream at the $(k+1)$th time step to the total number of aircraft present in the jth stream at the kth time step. This γ parameter is a key feature of the adaptive model: the γ parameters enable straightforward modeling of complex ATC actions like rerouting. Computation of all the model parameters is dealt with in detail in Sec. II.D. The next section discusses inputs to the baseline model-derivation process and input preprocessing.

B. Input to the Baseline Model-Derivation Process

The ETMS input file containing recorded track data in the Aircraft Situation Display to the Industry (ASDI) format is the input to the baseline model-derivation process. Data in this file are first preprocessed by running NASA's FACET [4] software in its playback mode, with the ETMS file as an input. FACET [4] is a software tool developed by NASA Ames Research Center. FACET provides a simulation environment for development and analysis of new air traffic management concepts. FACET, when run in playback mode, takes in track data from a recorded ETMS file and sends it to the graphical user interface (GUI) display. FACET can be customized to write, in parallel, the formatted position, velocity, and flight plan information into a TRX (TRACK) file while running in the playback mode. Format of such a TRX file is explained in the next paragraph.

The FACET TRX file has two types of entries. The TRACK_TIME entry gives the time at which the data that follows this entry is recorded. The time is given in seconds since 00:00:00 Coordinated Universal Time (UTC) on 1 January 1970. For each TRACK_TIME entry, there are one or multiple TRACK entries following it. Each TRACK entry corresponds to an aircraft that was airborne at that time. The format of the TRACK entry is as follows: TRACK is the aircraft identifier, aircraft-type, current latitude, current longitude, current speed, current flight level, current heading, current center, current sector, the string "FP_ROUTE,"and the filed flight plan for an aircraft as a sequence of waypoints starting with the origin airport and ending with the destination airport. (Names of the waypoints are separated by dots.)

At the University of Cincinnati, we have developed a software tool that reads position, velocity, and flight plan data from a TRX file and develops a baseline Eulerian model for the airspace under consideration, using this data, for a given time period. The start and end times for the modeled time period can be input into the software. In real time, this baseline model will be adapted using certain rules (to be stated later). These rules will specify how to modify the baseline model on the basis of differences in sector counts and flight plans between the baseline data and the real data obtained by online measurements. The next section explains the derivation of this baseline Eulerian model.

C. Derivation of Conservation Equations for a Single Stream of Aircraft

As explained before, track information for all aircraft within the ZFW center and its neighboring centers, for the required time period, is processed through FACET and stored in a TRX file. This file is read by our software, and Eulerian model parameters are computed by keeping track of inflows/outflows and departures/arrivals in each control volume. The following notation will be helpful in understanding the model-derivation process.

Notations: $\aleph(i)$ is the set of control volumes that are immediate neighbors of the control volume, to which stream i belongs. The term $n^{(i)}(k)$ is the number of aircraft present in the ith stream at time step k. The term $\alpha^{(i,i)}(k)$ is the ratio of the number of aircraft that remain behind in the ith stream after one discrete time interval from time step k to the number of aircraft present in the ith stream at time step k. The term $y_{\text{out}}^{(i)}(k)$ is the output rate in aircraft per minute going into the ith neighboring control volume. The term $y_{\text{in}}^{(i)}(k)$ is the input rate in aircraft per minute coming into the control volume from its ith neighboring control volume. The term $\gamma^{(i,j)}(k)$ is the ratio of the

Table 1 Fort Worth center sector connectivity table

Sector	Stream number	Associated high sector	State vector index
(High)			
Control volume no. 1; sectors included: ZFW46, ZFW15, ZFW16, ZFW17, ZFW96,	1	ZFW48	1
ZFWDF, ZFW97, ZFW98, ZFWAC, ZFW20, ZFW25	2	ZFW90	2
	3	ZFW71	3
	4	ZFW89	4
	5	ZFW65	5
	6	ZFW39	6
	7	ZFW94	7
	8	ZFW47	8
	9	ZHU	9
	10	Airports	10
Control volume no. 2; sectors included: ZFW48, ZFW53, ZFW36, ZFW37,	1	ZFW47	11
ZFW24, ZFW26, ZFW38, ZFW23, ZFWFS	2	ZFW42	12
	3	ZFW46	13
	4	ZFW49	14
	5	ZFW50	15
Control volume no. 3; sectors included: ZFW42	1	ZFW48	16
	2	ZFW90	17
	3	ZFW50	18
	4	ZME	19
Control volume no. 4; sectors included: ZFW90, ZFW27, ZFW83	1	ZFW46	20
	2	ZFW42	21
	3	ZFW71	22
	4	ZFW28	23
	5	ZME	24
	6	Airports	25
Control volume no. 5; sectors included: ZFW71	1	ZFW46	26
	2	ZFW90	27
	3	ZFW28-86-92	28
	4	ZFW89	29
Control volume no. 6; sectors included: ZFW89, ZFW29, ZFWGG, ZFW01	1	ZFW46	30
	2	ZFW71	31
	3	ZFW86	32
	4	ZHU	33
	5	Airports	34
Control volume no. 7; sectors included: ZFW28, ZFW92, ZFW86,	1	ZFW71	35
ZFW30, ZFWML, ZFWBD	2	ZFW90	36
	3	ZFW89	37
	4	ZHU	38
	5	ZME	39
	6	Airports	40
Control volume no. 8; sectors included: ZFW65, ZFW62, ZFWGR	1	ZFW82	41
	2	ZFW39	42
	3	ZFW46	43
	4	ZHU	44
	5	Airport SEP	45
Control volume no. 9; sectors included: ZFW39, ZFW32, ZFWAB	1	ZFW82–93	46
	2	ZFW94	47
	3	ZFW46	48
	4	ZFW65	49
Control volume no. 10; sectors included: ZFW94	1	ZFW93	50
	2	ZFW47	51
	3	ZFW46	52
	4	ZFW39	53
Control volume no. 11; sectors included: ZFW47, ZFW34, ZFWSP, ZFW75	1	ZFW93	54
	2	ZFW46	55
	3	ZFW94	56
	4	ZFW48	57
	5	ZFW49	58
	6	ZAB97	59
Control volume no. 12; sectors included: ZFW93, ZFW82, ZFW40, ZFW63,	1	ZFW47	60
ZFW64, ZFW43, ZFWMA, ZFWLT	2	ZFW94	61
	3	ZFW39	62
	4	ZFW65	63
	5	ZHU	64
	6	ZAB	65
	7	Airports	66

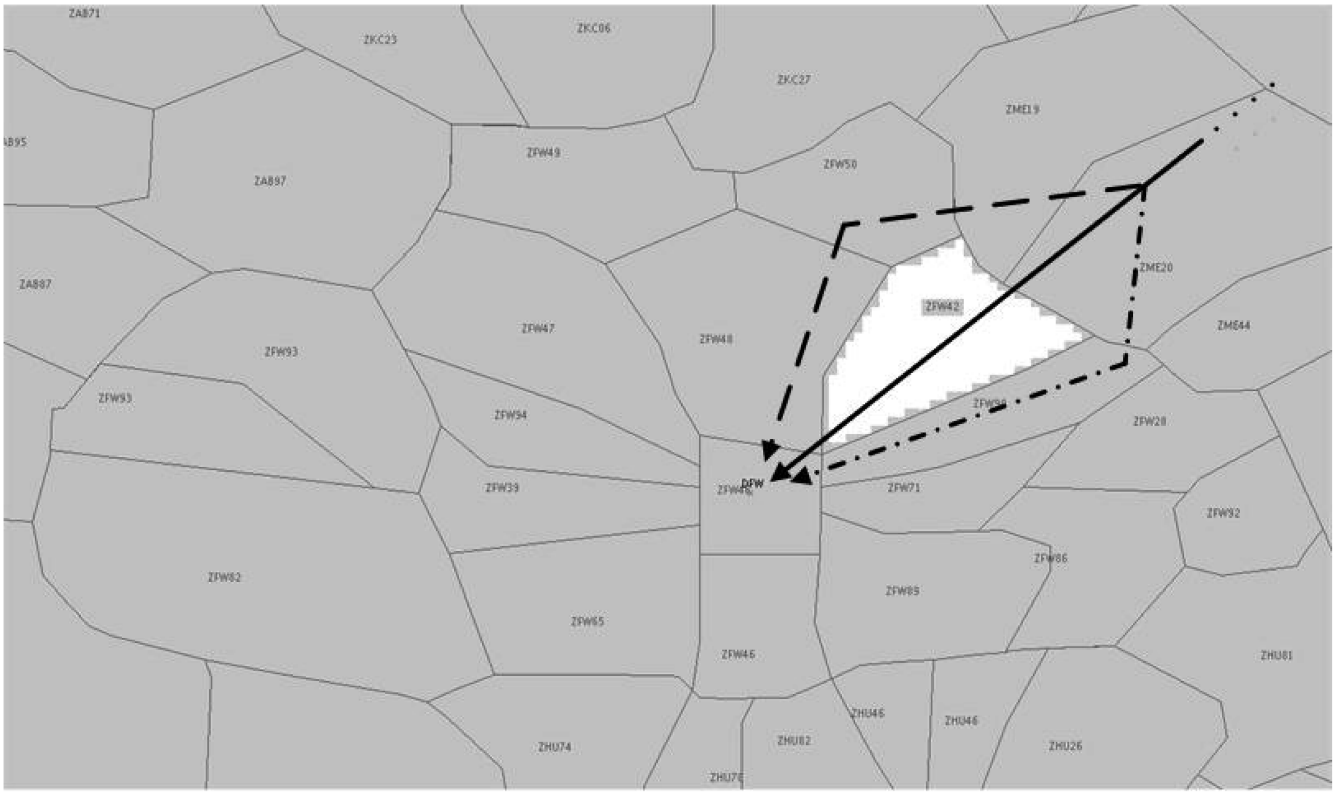

Fig. 2 Fort Worth center airspace, showing the high-level sectors.

number of aircraft present in the jth stream that change over to the ith stream during the kth time interval to the number of aircraft present in the jth stream at time step k. $\beta^{(i,j)}(k)$ is the ratio of aircraft coming into the control volume from its jth neighboring control volume and going into its ith stream to the total number of aircraft coming into the control volume through its jth neighboring control volume during the kth time interval. The term $u^{(i)}(k)$ is the ATC hold-back rate prescribed for the ith stream during the kth time interval. The term $q^{(i)}(k)$ is the departure rate for aircraft taking off from airports within the control volume and going into the ith stream. The term $s(i)$ is the total number of streams present in the control volume, to which the ith stream belongs. Finally, ΔT is the Eulerian model discrete time interval (1 min for the purpose of this modeling exercise).

Table 1 lists the 12 control volumes in the ZFW airspace and the corresponding streams. For example, streams no. 1 through no. 10 belong to the first control volume, whereas streams no. 61 through no. 66 belong to the last (twelfth) control volume. There are a total of 66 streams. Each control volume has 4 to 10 streams in it. Table 1 also lists the streams within each control volume and gives the adjacent control volumes with which each these streams are associated. Using the symbols introduced above, the flow of aircraft in the ith stream can be written as

$$n^{(i)}(k+1) = \alpha^{(i,i)}(k)n^{(i)}(k) + \sum_{j=1,j\neq i}^{s(i)} \gamma^{(i,j)}(k)n^{(j)}(k) + \Delta T \sum_{j\in\aleph(i)} \beta^{(i,j)}(k)y_{\text{in}}^{(j)}(k) + \Delta T u^{(i)}(k) + \Delta T q^{(i)}(k), \qquad i = 1, 2, \ldots, 10 \tag{1}$$

That is, the number of aircraft present in the ith stream at time step $k+1$ is equal to the ratio $\alpha^{(i,i)}(k)$ of the number of aircraft present in the same stream at the time step k, plus the number of aircraft changing over to the ith stream from other streams within the same control volume, plus the number of aircraft coming into the ith stream from adjacent control volumes, plus the aircraft held back by the ATC control actions, plus the aircraft coming into the stream through the unmodeled neighboring center(s) during the time interval $k\Delta T$ to $(k+1)\Delta T$.

Now, the outflow rate from the ith stream can be written as

$$y_{\text{out}}^{(i)}(k) = \frac{1}{\Delta T}\left[1 - \alpha^{(i,i)}(k) - \sum_{j=1,j\neq i}^{s(i)} \gamma^{(j,i)}(k)\right]n^{(i)}(k) - u^{(i)}(k), \qquad i = 1, 2, \ldots, 10 \tag{2}$$

That is, the outflow rate (aircraft per minute) is equal to the number of aircraft expected to go out of the stream (either to an adjacent control volume or to another stream within the same control volume or to external unmodeled airspace) minus the number of aircraft held back by the ATC control actions. Stream i is associated with one adjacent control volume. So, these aircraft go out into the adjacent control volume associated with stream i. At the next time step, these aircraft are assigned streams in the adjacent control volume, depending on the subsequent next control volume to which they would transit.

D. Computation of Parameters of the Eulerian Model

We derive the modeling parameters α, β, and γ from the recorded position, velocity, and flight plan data stored in the FACET TRX file. We explain this derivation process in the context of the control volume no. 1, which consists of the high-level sector ZFW46 and some low-level sectors. (Note: the first 10 streams belong to control volume no. 1.)

1. Computation of the Parameters $\alpha^{(i,i)}(k)$

1) Among all the aircraft present in the control volume ZFW46 at the time step k, pick those which will enter the ith adjacent control volume in the future (i.e., aircraft belonging to the ith stream). Let N_i be the number of such aircraft. [Aircraft that are supposed to land at an airport within the sector are classified into stream no. 10 for this control volume. So, if an aircraft is supposed to land at an airport within ZFW46, then it is assigned to stream no. 10 and will feature in the computation of $\alpha^{(10,10)}(k)$.]

2) Among these N_i aircraft, find the aircraft that remain behind in the same control volume and the same stream after the passage of one time step, that is, at time step $(k+1)$. Let this number be M_i.

3) Then, we have $\alpha^{(i,i)}(k) = M_i/N_i$.

2. Computation of the Parameters $\beta^{(i,j)}(k)$

1) Pick aircraft present in the adjacent control volume, associated with the jth stream, at time step k. Then, among these aircraft, pick those that move to the current control volume at time step $k+1$. Let the number of such aircraft be N_{in}.

2) Out of these N_{in} aircraft, pick those aircraft that are expected to enter the ith stream of ZFW46. Let the number of such aircraft be N_{in}^i.

3) Then $\beta^{(i,j)}(k) = N_{\text{in}}^i/N_{\text{in}}$.

3. Computation of the Parameters $\gamma^{(i,j)}(k)$

1) Pick the aircraft in sector ZFW46 belonging to the jth stream at time step k. Let $N1$ be the number of such aircraft.

2) Among these aircraft, pick the aircraft that switch over to stream i at time step $(k+1)$. Let $N2$ be the number of such aircraft.

3) Then, we have $\gamma^{(i,j)}(k) = N2/N1$.

Computation of parameters associated with other control volumes is done in a similar manner.

E. Derivation of the Eulerian Model for the Entire Airspace

The state variables of the Eulerian model are the aircraft counts in each of the individual streams in the control volumes present within the airspace under consideration. Table 1 lists the 12 control volumes in the ZFW airspace; each control volume has 4 to 10 streams in it. This table also lists the streams within each control volume and gives the adjacent control volumes with which each these streams are associated. There are a total of 66 streams in the model. The control inputs for this model are the ATC hold-back rates in each of these streams or a subset of the streams. The external inputs are the inflow rates coming from external regions, namely, the neighboring centers. Table 2 lists the external inflows and shows from where these inflows come and which ZFW sector they enter. There are a total of 14 external inputs. The state vector, control input vector, and the external input vector for the Eulerian model of this airspace are

$$\mathbf{X}(k) := [n^{(1)}(k), n^{(2)}(k), \ldots, n^{(66)}(k)]^T \tag{3}$$

$$\mathbf{U}(k) := [u^{(1)}(k), u^{(2)}(k), \ldots, u^{(66)}(k)]^T \tag{4}$$

$$\begin{aligned}\mathbf{D}(k) := \Big[& y_{zhu}^{\text{cv1}}(k), y_{zkc}^{\text{cv2}}(k), y_{zme}^{\text{cv2}}(k), y_{zkc}^{\text{cv3}}(k), y_{zme}^{\text{cv3}}(k), y_{zme}^{\text{cv4}}(k), \\ & y_{zhu}^{\text{cv6}}(k), y_{zhu}^{\text{cv7}}(k), y_{zme}^{\text{cv7}}(k), y_{zhu}^{\text{cv8}}(k), y_{zkc}^{\text{cv11}}(k), y_{zab}^{\text{cv11}}(k), \\ & y_{zhu}^{\text{cv12}}(k), y_{zab}^{\text{cv12}}(k) \Big]^T\end{aligned} \tag{5}$$

Here, $y_{z_{\text{ext}}}^{\text{cv}i}(k)$ represents the number of aircraft coming in from the external center z_{ext} into the ith control volume during the kth time step. These uncontrolled inputs map to the $q^{(i)}(k)$ terms in Eq. (1). For example, the inflow from Houston center to control volume no. 1 is associated with stream no. 9. So, we have $q^{(9)}(k) = y_{zhu}^{\text{cv1}}(k)$.

Using the state variables $n^{(i)}(k)$, control inputs $u^{(i)}(k)$, and external (uncontrolled) inputs $q^{(i)}(k)$, conservation relations similar to Eqs. (1) and (2) can be written for each stream within each control volume. In vector notations, the conservation relations for the entire ZFW center can be written in a compact form as

$$\mathbf{X}(k+1) = A_k\mathbf{X}(k) + B_k\mathbf{U}(k) + G_k\mathbf{D}(k) \tag{6}$$

where,

$$A_k(i,j) = \begin{cases} \alpha^{(i,i)}(k) & \text{if } i = j \\ \gamma^{(i,j)}(k) & \text{if } j \in \text{control}_{\text{volume}}(i),\ j \neq i \\ \beta^{(i,j)}(k)\{1 - \alpha^{(l,l)}(k) - \displaystyle\sum_{m \in \text{control}_{\text{volume}}(l)} [\gamma^{(m,l)}(k)]\} & \text{if } l \in \aleph(j) \end{cases} \tag{7}$$

$$B_k(i,j) = \begin{cases} 1 & \text{if } i = j \\ \beta^{(i,j)}(k) & \text{otherwise} \end{cases} \tag{8}$$

$$G_k(i, n_q) = \beta^{[i,\text{stream}(n_q)]}(k) \quad \text{for } n_q = 1, 2, \ldots, 14 \tag{9}$$

where $\text{stream}(n_q)$ refers to the stream number associated with the external inflow n_q, and $\text{control}_{\text{volume}}(i)$ is the set of all streams that belong to the same control volume as stream i.

Table 2 External inflows

External inflow number	Coming from sector	Going into sector
No. 1	ZHU78, ZHU82, ZHU83	ZFW46
No. 2	ZFW49, ZFW35	ZFW48
No. 3	ZFW50, ZFW38	ZFW48
No. 4	ZFW50, ZFW38	ZFW42
No. 5	ZME19, ZME20, ZME22, ZME44, ZME43, ZME66, ZME67, ZME01, ZME02	ZFW42
No. 6	ZME19, ZME20, ZME22, ZME44, ZME43, ZME66, ZME67, ZME01, ZME02	ZFW90
No. 7	ZHU46, ZHU26, ZHU81, ZHU86, ZHU38, ZHU40	ZFW89
No. 8	ZHU46, ZHU26, ZHU81, ZHU86, ZHU38, ZHU40	ZFW28-86-92
No. 9	ZME19, ZME20, ZME22, ZME44, ZME43, ZME66, ZME67, ZME01, ZME02	ZFW28-86-92
No. 10	ZHU74, ZHU97, ZHU50	ZFW65
No. 11	ZFW49, ZFW35	ZFW47
No. 12	ZAB97, ZAB87, ZAB23, ZAB78	ZFW47
No. 13	ZHU74, ZHU97, ZHU50	ZFW82-93
No. 14	ZAB97, ZAB87, ZAB23, ZAB78	ZFW82-93

Explanation of the matrix entries: Each diagonal entry of the A matrix relates the aircraft count at the current time step with the aircraft count at the next time step for the same stream. Hence, the diagonal entries are set equal to the retention ratios $\alpha^{(i,i)}(k)$.

Aircraft may "jump" from one stream to another within the same control volume if there is a change in the aircraft's route or flight plan. These jumps are captured by the $\gamma^{(i,j)}(k)$ parameters. These parameters are a key feature of the adaptive model because they enable easy modeling of complex ATC actions like rerouting. In the ith row of the A matrix, the entries corresponding to streams belonging to the same control volume as the ith stream are set equal to the corresponding $\gamma^{(i,j)}(k)$ value. For example, referring to Table 1, we see that stream no. 24 belongs to the control volume associated with sector ZFW90. The set of streams belonging to this control volume is $\{20, 21, \ldots, 25\}$. So, in the 24th row of the A matrix, entries belonging to columns $\{20, 21, 22, 23, 25\}$ will have the values $\gamma^{(24,j)}(k)$, $j = 20$, 21, 22, 23, and 25, respectively, to depict aircraft transfers within the streams belonging to ZFW90's control volume caused by reroutes or flight plan changes.

Each stream in a given control volume also gets inflows from all neighboring control volumes. Consider two adjacent control volumes $C1$ and $C2$. Suppose the lth stream of control volume $C2$ is associated with control volume $C1$, and the jth stream of control volume $C1$ is associated with the control volume $C2$. The outflow from $C2$ to $C1$ will be equal to the number of aircraft present in stream l minus the number expected to remain back in the same stream minus the number of aircraft that change over to other streams within control volume $C2$. A ratio $\beta^{(i,j)}(k)$ of this number will go into the ith stream of control volume $C1$. So, in the ith row of the A_k matrix, the entries corresponding to lth stream in control volume $C2$ will be assigned the value $\beta^{(i,j)}(k)\{1 - \alpha^{(l,l)}(k) - \sum_{m \in \text{control}_{\text{volume}}(l)}[\gamma^{(m,l)}(k)]\}$. For example, stream no. 2 belongs to control volume no. 1, and it is associated with the flow between the control volumes no. 1 and no. 4. Suppose there is an aircraft going from control volume no. 4 to control volume no. 1 and thereafter continuing on to control volume no. 8, which is associated with stream no. 5 of control volume no. 1. In control volume no. 4, flow to control volume no. 1 is associated with its first stream (which is stream no. 20 in the model). So, in effect, the aircraft is transitioning from stream no. 20 to stream no. 5. Hence, the entry (5, 20) of the A_k matrix would be set to $\beta^{(5,2)}(k)[1 - \alpha^{(20,20)}(k) - \sum_{m \in \text{cv4}} \gamma^{(m,20)}(k)]$.

Finally, a stream may get inflows from the neighboring (unmodeled) centers. The inflow from a particular external center to a control volume is given by the corresponding entry of the $D(k)$ vector. A ratio $\beta^{(i,j)}(k)$ of this inflow will enter the ith stream of the control volume (the jth stream corresponds to the adjacent unmodeled region). Stream(n_q) gives this stream number associated with the external inflow n_q. There are 14 external inflows coming into the modeled airspace from outside. The details of these flows are given in Table 2. The corresponding stream number can be read from Table 1. Hence, in the ith row of the G_k matrix, entries corresponding to streams that get external inflows are assigned the values $\beta^{[i,\text{stream}(n_q)]}(k)$. For example, the first external inflow is the flow from Houston center into ZFW46's control volume. From Table 1, the stream number for this external inflow is 9. So, the $\beta^{(j,9)}(k)$, $j = 1, 2, \ldots, 10$ entry (the first 10 streams are associated with ZFW46's control volume) will be nonzero if some aircraft coming into ZFW46 from Houston center enter that particular stream j.

F. Validation of the Eulerian Model Against Baseline Data

To validate the baseline Eulerian model derived thus far, we compare sector count predictions of the Eulerian model with the sector counts obtained by running FACET in the playback mode using the same track data. The process of validation is better explained in Fig. 3. For the comparison results presented here, we used a time period of 1 h starting from 05:00:00 GMT to 05:59:00 UTC on 13 March 2005. The ETMS track data for this period was used to derive the baseline Eulerian model. For the purpose of model validation, FACET was run in playback mode using the same ETMS (ASDI format) input file for the same time period, and aircraft counts for all the control volumes present in the ZFW center were stored at 1 min time intervals. Also, starting with the same initial sector counts at 04:59:00, the Eulerian model was iterated, and control volume count predictions were obtained. Figure 4 shows aircraft count prediction comparison for the first four control volumes. The unbroken line with square markers shows the actual baseline sector counts obtained by running FACET in the playback mode, whereas the dotted line with star-shaped markers shows the Eulerian model predictions. This figure shows that the Eulerian model exactly predicts sector counts for the first four control volumes. Exact aircraft count predictions were obtained for the other eight control volumes, too. Baseline Eulerian model derivation was done using ETMS data for other time periods, too. The model derivation and validation process was repeated for a number of other time periods. It was observed that baseline Eulerian models derived for other time periods, using the same method, proved to be exact in their sector count predictions too.

III. Adaptation of the Baseline Eulerian Model to Real Data

In this section, we answer the following questions: Can the Eulerian model that we derived in the last section using recorded air

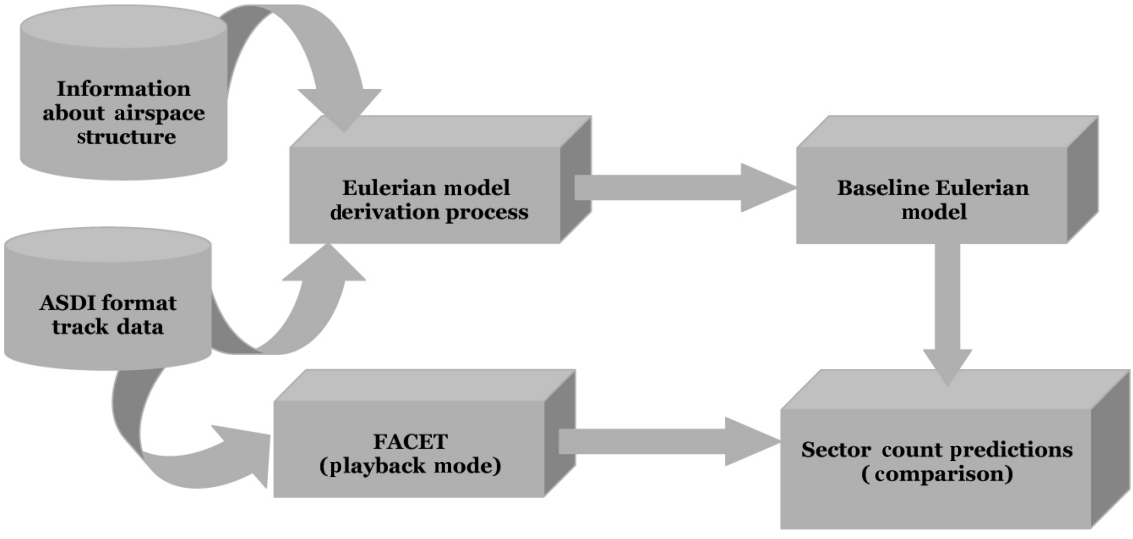

Fig. 3 Validation of the baseline Fort Worth center Eulerian model.

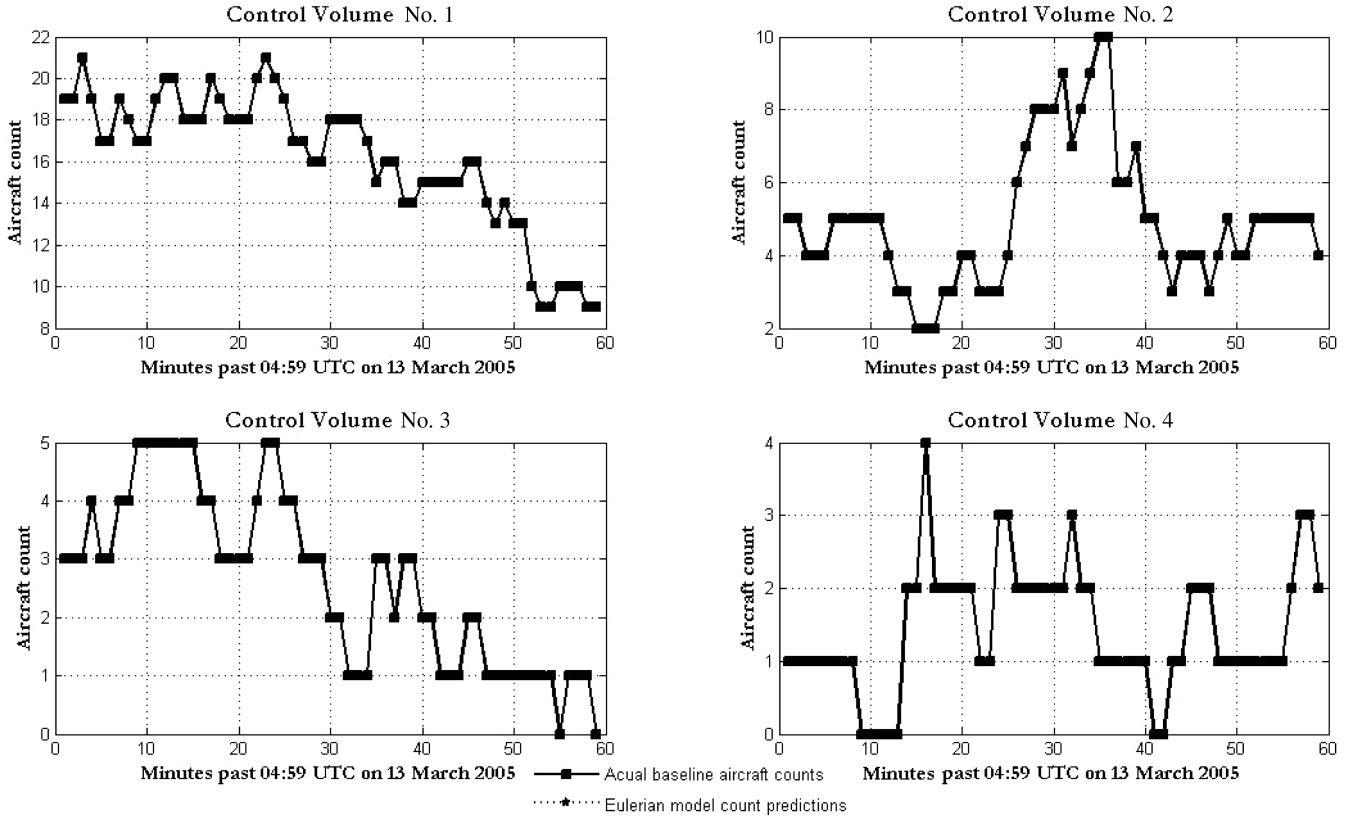

Fig. 4 Comparison of the Eulerian model sector count predictions and the baseline control volume counts.

traffic data for a given time period be adapted and used to predict sector counts in the ZFW center for any other time period? In particular, can it be adapted to predict sector counts in real time, accurately? Because the number of aircraft present in any part of an airspace is a complex function of the day of the week, the time of the day, the weather, and many other factors, it is not feasible to use the Eulerian model derived using historical data directly for real-time sector count prediction. However, if we have an Eulerian model derived using recorded/historical data for a given airspace, then depending upon differences in the flight plans between the current time and the time for which the Eulerian model is derived, the Eulerian model can be adapted online to make accurate real-time predictions.

In practice, a baseline Eulerian model can be derived offline, for the whole NAS, one day in advance. This can be done using ahead-of-time information about the flight schedules and the predicted weather. An air traffic simulation software like FACET can be used to integrate aircraft trajectories using this information and to get the track data needed for deriving the baseline model. The baseline model represents what is expected to happen based on prior knowledge of the flight plans and weather. As the day progresses, differences in the baseline and real-time traffic situations can be used to adapt this model online. Then, in real time, as the traffic/weather situation develops, the baseline model will get adapted and become more "current." Because of its low dimensionality and easy adaptability, such a model can be used in simulation-based optimization schemes for fast computation of optimal rerouting, metering, and ground-hold decisions. The following paragraphs and subsections explain how online model adaptation can be achieved.

There are some principles that we use while adapting the baseline model:

1) If additional aircraft other than those present in the baseline traffic are present in the real-world traffic, then these additional aircraft will be assumed to follow nominal routes between their origin and destination airports.

2) When we add or remove aircraft from the baseline model to make it emulate the real-time traffic situation, we need information on the nominal control volume transit times for those aircraft. We assume that the nominal control volume transit times for frequently traveled routes are known. These may be approximated by average transit times computed from historical data. Control volume transit times may differ depending upon the direction of travel. For example, it may take more time for traversing the control volume containing sector ZFW42 in the east-to-west direction than traversing the same control volume in the north-to-south direction. Detailed information about nominal control volume transit times for each stream within each control volume is necessary for making accurate adaptations to the baseline model.

3) Usually, there will be some real-world aircraft, which follow the same routes in real time as in the baseline situation. The stream retention ratio parameters $\alpha^{(i,i)}(k)$, branch parameters $\beta^{(i,j)}(k)$, and interstream transition parameters $\gamma^{(i,j)}(k)$ of the baseline model will be modified to keep the transition of such aircraft from one control volume to the next unchanged from the baseline situation, despite the extra/fewer aircraft present.

4) The branch parameters $\beta^{(i,j)}(k)$ of the baseline model will be changed depending upon the differences in the number of aircraft coming into a particular stream from a given adjacent control volume in the baseline model versus the real world. For example, in the control volume associated with sector ZFW46, the adjacent control volume, ZFW48, corresponds to the first stream. If, in the baseline model, two aircraft come into ZFW46 from ZFW48 in one time step, and out of those one aircraft goes into stream no. 5 and one aircraft goes into stream no. 3, then in the baseline model the parameters $\beta^{(5,1)}(k)$ and $\beta^{(3,1)}(k)$ will both have value 0.5, and the parameters $\beta^{(j,1)}(k)$, $j = 1, 2, 4, 6, 7, 8, 9$, and 10 will have value zero. If, in the real world, there are instead three aircraft coming into ZFW46 from ZFW48, with two aircraft going to ZFW65 and one going out to ZFW71, then, based upon this information, we can adapt the parameters $\beta^{(5,1)}(k)$ and $\beta^{(3,1)}(k)$ to have values $2/3$ and $1/3$, respectively.

5) If any rerouting decision has been taken in real time, then we could change the $\alpha^{(i,i)}$, $\beta^{(i,j)}$, and $\gamma^{(i,j)}$ parameters to depict this decision.

A. Example: Eulerian Model Adaptation

In the preceding section, we derived a linear time varying Eulerian model for the ZFW center for a period of 05:00:00 UTC to 05:59:00 UTC on 13 March 2005. In this section, we describe the process by which we adapt this model to make accurate predictions for some other day/time period if the air traffic on that day differs from that on 13 March 2005. Let us assume that on this other day all the traffic is following a similar pattern as on 13 March 2005, except that there are additional aircraft coming in from the northeast to DFW airport: one additional aircraft per five minutes. Nominally, an aircraft coming in from the northeast to DFW enters the ZFW center, from the neighboring Memphis center (ZME), through sector ZFW42. Then it travels through ZFW42 and crosses over to sector ZFW48. Finally, it enters sector ZFW46 and lands at the DFW airport. The nominal times spent by an aircraft on this route in each of the sectors ZFW42, ZFW48, and ZFW46 are known. Suppose we know beforehand that the first additional aircraft enters ZFW42 from neighboring center at 05:01:00, and thereafter, one additional aircraft enters ZFW42 every five minutes. Then, with this information about the differences in the baseline versus the real-world traffic situation, we can adapt the already-derived baseline model to make sector count predictions for this modified flow, without trajectory integrations, as follows.

Consider the first additional incoming aircraft, which enters the ZFW center at the boundary of sector ZFW42 with the ZME center. Suppose that this aircraft enters ZFW42 at time step $k1$ (ZFW42 is included in control volume no. 3, i.e., cv3). Then, it enters ZFW48 (cv2) from cv3 at time step $k2$, enters ZFW46 (cv1) from cv2 at time step $k3$, and finally lands at the DFW airport at time step $k4$. We know the nominal times spent by the aircraft in each of the sectors/control volumes. So, once we know $k1$, then $k2$, $k3$, and $k4$ can be computed from $k1$. The following changes will have to be made to the baseline model parameters to include this additional aircraft in the model. [Note that, in the following discussion, we have made slight changes to the notation: all parameters now carry a subscript, which specifies what control volume they refer to. This has been done to make it easier to understand the equations, without having to refer to Table 1 for stream numbers each time. So, now $\beta^{(i,j)}_{\mathrm{cv}m}(k)$ corresponds to the β parameter associated with streams i and j of the mth control volume.]

At the time step $k1$, the additional aircraft will enter the sector ZFW42 from the ZME center. So, we need to increment the incoming aircraft count for the ZME–ZFW42 external input (external input no. 5 in Table 2).

$$y^{\mathrm{cv3}}_{\mathrm{zme}}(k) = y^{\mathrm{cv3}*}_{\mathrm{zme}}(k) + 1 \tag{10}$$

Note that a $*$ on the name of a variable refers to the baseline value of that variable. Because this aircraft enters cv3 through stream 4 (associated with ZME center) and will leave it through stream 1 (associated with cv2), the corresponding branch ratio has to be updated to reflect one additional aircraft coming in.

$$\beta^{(1,4)}_{\mathrm{cv3}}(k) = \frac{[\text{baseline number of aircraft coming in from ZME to cv3 stream } 1 + 1]}{[\text{baseline number of aircraft coming in from ZME to cv3 all streams} + 1]} \tag{11}$$

The remaining branch ratios $\beta^{(j,4)}_{\mathrm{cv3}}(k)$, $j \neq 1$, must also be modified to take into consideration the additional aircraft coming in.

$$\beta^{(j,4)}_{\mathrm{cv3}}(k) = \frac{[\text{baseline number of aircraft coming in from ZME to cv3 stream } j]}{[\text{baseline number of aircraft coming in from ZME to cv3 all streams} + 1]}, \qquad j \neq 1 \tag{12}$$

Similar modifications to the respective α, β, and γ parameters have to be made at each of the time steps $k1$, $k1 + 1$, $k1 + 2, \ldots, k4$ to depict the travel of the additional aircraft as it travels through cv2, enters cv1, and finally lands at DFW airport. Model parameter changes for each additional aircraft will follow a similar pattern because the modeling equations are linear in sector aircraft counts. So, if more than one additional aircraft (over and above those in the baseline model) are predicted to enter the modeled airspace in the real-world situation, the previously described model adaptation process can be iteratively applied at the time instants when each aircraft is expected to enter the modeled region.

The model adaptation process presented here takes care of a simple scenario, wherein the baseline and real-world traffic situations differ only in terms of additional aircraft coming into the ZFW center through just one route. However, any complicated scenario, such as additional traffic coming in along multiple routes, weather-enforced closure of a particular sector, imposition of miles-in-trail restriction at a sector boundary, airport congestion due to change in airport configuration, etc., can be handled with similar ease due to the linear and additive nature of the model. Section III.B presents an example of the use of this adaptable model to simulate rerouting scenarios and its application to optimal rerouting decision making. The next section presents validation of the adapted model against real-world traffic data.

B. Validation of the Adapted Model

The real traffic situation considered in the previous example consists of some additional aircraft coming into ZFW from the northeast and landing at DFW over and above the baseline traffic on 13 March 2005. All other flights follow similar routes as in the baseline traffic. In the last subsection, we adapted the baseline Eulerian model to emulate this real traffic situation. To validate the adapted model, we compare the sector count predictions of this model with the actual sector counts obtained by running FACET in playback mode, using a TRX input file containing the additional flights [i.e., the same TRX file involved in the baseline model derivation is used; only one additional aircraft per five minutes traveling from La Guardia airport (LGA) to DFW is added to this file]. Note here that the adaptation process does not use aircraft trajectory integrations (i.e., track information). It only uses information about differences between the baseline and real flight plans for adapting the parameters of the baseline model. So, the adaptation process is very fast: it only involves the application of parameter modifications as in Eqs. (10–12).

To get the real sector counts, FACET was run in the playback mode with the additional aircraft included in its input TRX file for the period of 05:00:00 to 05:59:00 GMT. The sector counts for all ZFW sectors were stored at 1 min intervals. Then, starting with the same sector counts at the initial time 04:59:00 GMT, the adapted model was run to make sector count predictions for a period of 05:00:00 to 05:59:00 GMT. Figure 5 shows a comparison of the real sector counts and the baseline sector counts for the sectors affected by the additional aircraft, namely, control volumes no. 1, no. 2, and no. 3. The unbroken line with square markers shows the real sector counts, and the dotted line with star-shaped markers shows the baseline sector counts. It is seen that ten additional aircraft enter the modeled airspace over and above the baseline aircraft: seven aircraft land at airports in cv1 before the end of simulation (05:59:00), and, out of the remaining aircraft, one aircraft is airborne in cv1 and two are in cv3 at 05:59:00. It is clear from this figure that, if we use the baseline model for making sector count predictions in real time, the predictions will be far from accurate because the predictions will try to follow the

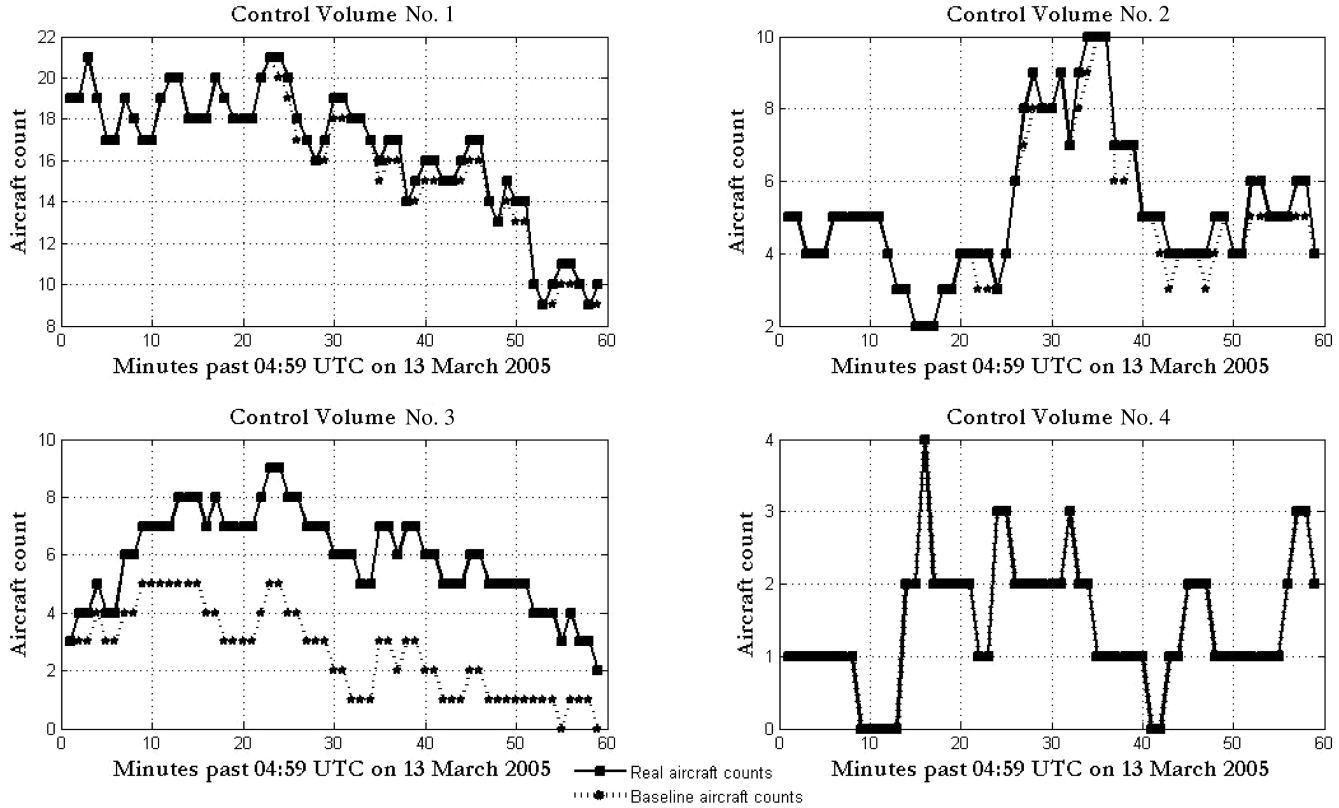

Fig. 5 Comparison of the real and baseline control volume counts.

baseline sector counts. Figure 6 shows a comparison of the real sector counts and the adapted model predictions. The unbroken line with square markers shows the real sector counts, whereas the dotted line with star-shaped markers shows the adapted model predictions of these sector counts. Again, it is seen from the plots that the adapted model predictions exactly match the real sector counts. This was possible because we had perfect information regarding the differences in the baseline versus the real time traffic situations.

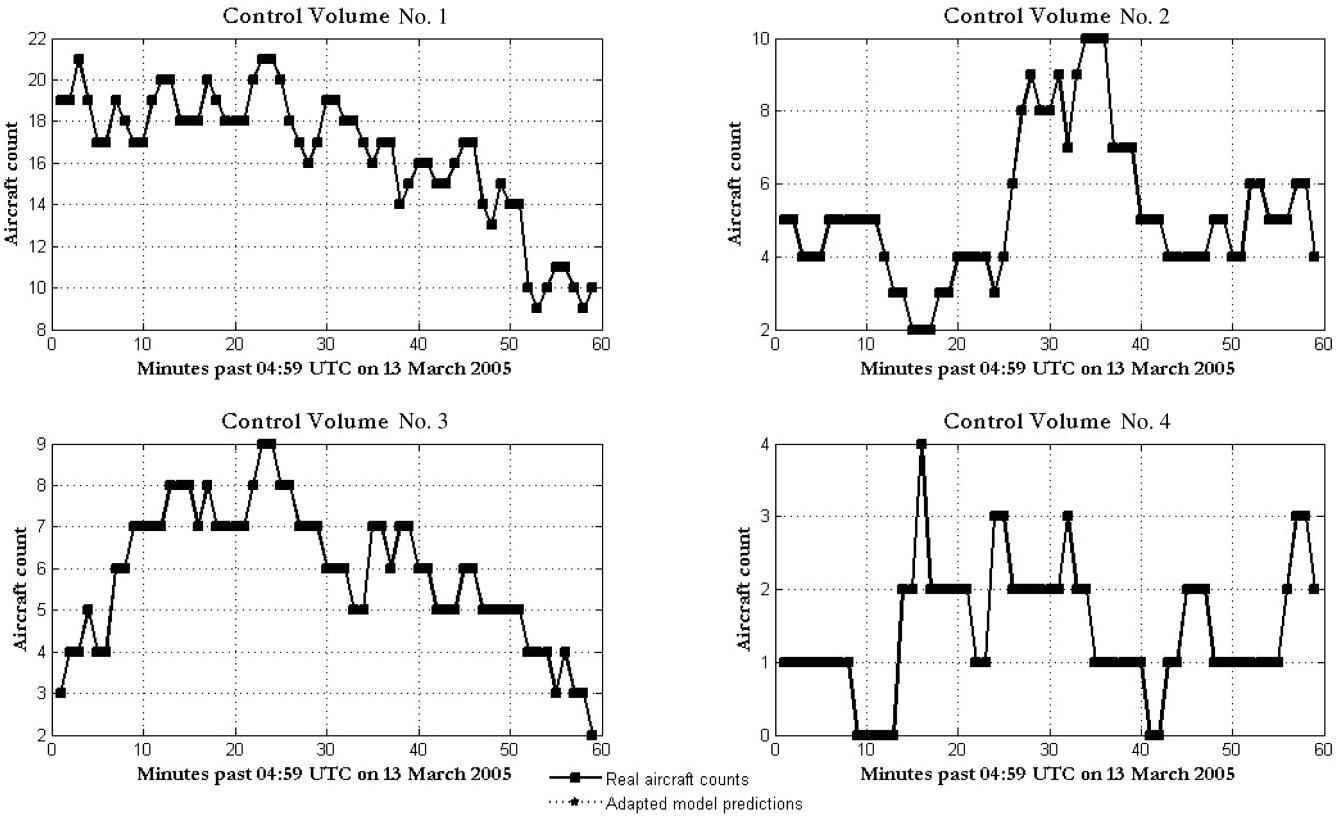

Fig. 6 Comparison of the real control volume counts and adapted model predictions of the sector counts.

IV. Simulation-Based Optimization for Air Traffic Flow Management

The preceding sections showed how we can derive a baseline Eulerian model for an airspace using recorded track data and then adapt this model online to match the real world. We showed that this model is capable of making accurate real time sector count predictions. Such a model is of high utility for air traffic flow management in the sense that if the model predicts that a particular sector will be overloaded in the future, then some control action (like change in miles-in-trail restriction, etc.) can be taken to keep the number of aircraft in that section down to a manageable level. The optimal ATC action to be taken can also be computed with the help of this model. In particular, because this model is of low dimensionality and because it is easily adaptable to simulate effects of different ATC actions, it can be used in an online simulation-based optimization scheme to evaluate the effects of different rerouting or metering strategies and then to select the best strategy. Additionally, this approach is highly flexible: the optimization cost can be configured to represent any one of a large number of different traffic management objectives. Figure 1 explains this simulation-based optimization process, pictorially. The optimization process chooses the best control action among a finite set of feasible actions. For each control action, changes are made to the real-time adapted Eulerian model to depict the effects of applying this control action. The model is iterated forward in time, and its predictions are used to compute the cost associated with the chosen control action. The control action, which gives the lowest cost, is chosen and applied to the real traffic.

In Sec. IV.B, we describe the use of simulation-based optimization for computing optimal rerouting strategies for a scenario in which an airspace region is closed due to severe weather. We use the adapted Eulerian model to make future sector count predictions as functions of the control inputs (rerouting commands). The optimal rerouting problem is then formulated as the minimization of a cost, which penalizes sector overload in the sectors that will carry the rerouted traffic. The minimization is done by using a stagewise network optimization algorithm rather than by formulating the problem as a mathematical program. The difficulty in formulating this problem as a mathematical program comes from the control-dependent nature of the Eulerian model, which will be discussed in the next section.

Table 3 Effect of nonzero hold-back controls on the model parameters (hold-back controls are zero here)

Sending stream	k	$k+1$	$k+2$	$k+3$
Number of aircraft	5	3	2	2
Outgoing aircraft	1	0	0	——
Aircraft changing stream	1	1	0	——
α	3/5	2/3	1	——
γ	1/5	1/3	0/2	——
Receiving stream	k	$k+1$	$k+2$	$k+3$
Number of aircraft	3	4	4	4
Incoming aircraft	1	0	0	——
α	1	1 (4/4)	1	——
γ	0/3	0/4	0/4	——
β (receiving stream, sending stream)	1	0	0	——

Table 4 Effect of nonzero hold-back controls on the model parameters [hold-back control $u(k) = 1$]

Sending stream	k	$k+1$	$k+2$	$k+3$
Number of aircraft	5	4	2	3
Outgoing aircraft	**0**	**1**	0	——
Aircraft changing stream	1	1	0	——
α	3/5	**2/4**	1	——
γ	1/5	**1/4**	0/2	——
Receiving stream	k	$k+1$	$k+2$	$k+3$
Number of aircraft	3	4	4	4
Incoming aircraft	0	**1**	0	——
α	1	**1 (3/3)**	1	——
γ	0/3	**0/3**	0/4	——
β (receiving stream, sending stream)	1	**1**	0	——

A. Control-Dependent Nature of the Eulerian Model

Control inputs to the Eulerian model are hold-back rates in different control volumes, that is, the number of aircraft held back in different control volumes per minute. The parameters of the Eulerian model corresponding to each stream of each control volume are 1) the stream retention parameter $\alpha^{(i,i)}(k)$, which is the ratio of the number of aircraft remaining back in the control volume at the next time step to the current stream aircraft count, 2) the interstream transition parameter $\gamma^{(i,j)}(k)$, which is the ratio of the number of aircraft transitioning from stream j to i within the same control volume at the next time step to the current number of aircraft in stream j, and 3) the branch ratio parameter $\beta^{(i,j)}(k)$, which is the ratio of aircraft coming into the control volume through stream j and going out through stream i to the total number of aircraft coming in through stream j at the time step k. If the hold-back control input associated with a particular stream of a control volume is nonzero, it means that at least one additional aircraft will be present in that stream at the next time step. Hence, at the next time step, the stream retention parameter for stream i, the stream transition parameters for all other streams within the same control volume as stream i, and the branch ratio parameters for the receiving stream of the adjacent control volume associated with stream i will have to be modified to depict this change.

Tables 3 and 4 elucidate this point. Consider two streams: a sending stream and a receiving stream. Table 3 depicts the situation when no aircraft is held back in the sending stream at time step k. In this case, the parameters α and γ of the sending stream have values 3/5 and 1/5, respectively, at time step k. This means that out of the five aircraft present in the stream at time k, one goes out to another stream within the same control volume, and one goes out of the control volume to the receiving stream, leaving three aircraft in the sending stream at time step $k+1$. Values of the α and γ parameters are 2/3, 1/3 at time step $k+1$ and 1, 0 at time step $k+2$. So, this leaves two aircraft in the sending stream at time steps $k+2$ and $k+3$, with no aircraft going out to the receiving stream. The receiving stream has α parameter of value 1 and γ parameter of value 0 for all time steps. So, it starts with three aircraft at time step k, gets the additional aircraft at $k+1$, and from there onward has four aircraft in it at $k+1$, $k+2$, and $k+3$.

Table 4 depicts the situation when one aircraft is held back in the sending stream at time step k. In this case, there is one additional aircraft in the sending stream, and one fewer aircraft in the receiving stream at time step $k+1$. Hence, the α and γ parameters for both the streams for time step $k+1$ have to be modified as shown in Table 4. Note that if we did not take into consideration the control-dependent nature of the model and kept all the model parameters unchanged, then with a nonzero hold-back control input, the sending stream equations would look like the following. At time step k: $n(k) = 5$. At time step $(k+1)$: $n(k+1) = (3/5) \times 5 + 1 = 4$. At $(k+2)$: $n(k+2) = (2/3) \times 4 = 8/3$. The number of aircraft going out from the sending stream to the receiving stream at $k+2$ will be $n_{\text{out}}(k+2) = [1 - (2/3)] \times 4 = 4/3$. Finally, at $(k+3)$: $n(k+3) = 1 \times (4/3) = 4/3$. The stream aircraft counts in this case are not only incorrect, they are also fractional. Similarly, for the receiving stream, keeping model parameters unchanged would mean that the model will predict four aircraft in that stream at time step $k+1$, which is incorrect; it should have only three aircraft at $k+1$ because one aircraft is held back in the sending stream for that time step.

The actual Eulerian model consists of a complicated interconnection of such sending and receiving streams. The simple example here shows why the Eulerian model parameters are control dependent. Most previous works related to the use of Eulerian models in ATM do not consider this control dependence. In our work, we build on these previous works, especially Menon et al. [7–10], which are seminal works in the area of the use of Eulerian models

in ATM, and we take a further step by acknowledging the control-dependent nature of the Eulerian model while formulating the model-based optimization problem. To this end, we modify the model-based optimization process by adapting the Eulerian model to depict control action effects whenever a particular control input is nonzero. Taking into consideration the control dependence of the Eulerian model in making predictions is a nontrivial contribution of our work.

Because of the control-dependent nature of the Eulerian model, we cannot formulate the model-based optimization as a mathematical program because the model has to be modified to depict control action effects whenever a particular control input is nonzero. Instead, we search for the optimum control by doing a stagewise search over the set of all possible control values. For each distinct control value that we consider, we make the requisite model adaptations and iterate the adapted model until the end of the prediction horizon to compute the final value of the optimization cost associated with that control value. The following section sets up the optimization problem in terms of its objectives, controls, and constraints.

B. Use of the Eulerian Airspace Model for Making Optimal Rerouting Decisions

Quite often, bad weather in some parts of the NAS reduces the capacity of some sectors, sometimes even to zero. In such cases, controllers in adjoining sectors have to compute alternate routes to take the aircraft around this closed sector/region. Generally, there are multiple alternate routes that the controllers can choose from. For example, if a sector carrying east-to-west air traffic is closed down, then the controller in the adjoining eastern sector may have the freedom to reroute the aircraft via a sector north of the closed sector or a sector south of the closed sector; or, he/she may reroute some aircraft via the northern sector and some aircraft via the southern sector. In some scenarios, a sector adjoining the closed airspace may be carrying unidirectional flows, and the controller may not be allowed to reroute too many aircraft through this sector if they are going in the opposite direction as the main sector traffic. This is especially true for sectors near a major airport: such sectors are generally dedicated to unidirectional flows: either arrivals to or departures from the nearby major airport. Thus, in many cases, computing the optimal rerouting policy is not trivial. Currently, when weather closes down some parts of the NAS, the Air Traffic Control System Command Center (ATCSCC) initiates an iterative negotiation process with the Airline Operations Centers (AOCs) to decide on the best rerouting and rescheduling policy so as to minimize weather-related delays. The ATCSCC first informs each airline's AOC about the need for rerouting around a weather-affected region. Each AOC then generates new flight plans, for all its scheduled flights, that it would like them to follow by taking into consideration fuel, delay, and safety costs, and then it sends them to the ATCSCC. The ATCSCC reviews the new flight plans for all airlines and accepts them or suggests revision. This collaborative decision-making process is based on the experience of the air traffic controllers and personnel at the ATCSCC and the AOCs. Hence, this process may lead to suboptimal rerouting decisions, and millions of dollars may be lost in the form of fuel and delay costs. A formal optimization scheme based on accurate traffic flow predictions can be used to overcome the drawbacks of this decision-making process. In this section, we demonstrate how our adaptive Eulerian airspace model can be used to make optimal rerouting decisions.

We look at the following rerouting scenario: We assume that sector ZFW42 (shown in white in Fig. 2) is closed due to bad weather. The primary flow in this sector (shown by the unbroken arrow in Fig. 2) consists of aircraft coming from the neighboring Memphis center and crossing over to sector ZFW48 first and then to the central ZFW sector, sector ZFW46, to land at one of the airports within this sector. We assume that the aircraft that are already present in sector ZFW42 when it is closed down are allowed to go on along their preplanned routes. However, once sector ZFW42 is closed, all aircraft that are supposed to enter ZFW42 from the ZME center in the future are rerouted around this closed sector. For each aircraft affected by this sector closure, there are two alternate routes that it can take. It can either take a northern route (the dashed arrow in Fig. 2), which takes it through the part of ZME north of ZFW42, then through sector ZFW50, then on to sector ZFW48, and finally to the central sector ZFW46, where it lands at its destination airport. Or the affected aircraft may take a southern route (the dash–dot arrow in Fig. 2), entering ZFW through sector ZFW90, passing all the way through ZFW90 to enter ZFW46, and then landing at its destination airport within ZFW46. If all the aircraft are rerouted via one of the above two reroute paths, then this may result in sector overload for some sectors along the chosen reroute path. Additionally, sectors along the reroute paths may be getting aircraft from other sources, too. So, making rerouting assignments based just on the relative capacities of sectors on alternative reroute paths may not be optimal. The rerouting strategy has to manage reroute assignments in such a way that aircraft counts in these sectors do not go over their maximum allowable values because of the aircraft that the rerouting would be adding on top of the aircraft already coming in to these sectors through other sources. So, the decision that the controller has to make is not only how many aircraft to reroute through the northern route and how many aircraft through the southern route, but also which of the incoming aircraft to reroute through the either alternative routes (because different aircraft will enter the sectors at different times and may cause sector overloads depending upon when the sectors get aircraft from the other sources). This is a nontrivial optimization problem. In the following paragraphs, we describe how simulation-based optimization using Eulerian model predictions can be used to compute the optimal rerouting policy.

C. Greedy Algorithm for Computing the Optimal Rerouting Policy

In this section, we present a greedy algorithm for computing the optimal rerouting policy and demonstrate its working using the ZFW42 sector closure example. A greedy algorithm is any algorithm that follows the problem-solving metaheuristic of making the locally optimum choice at each stage with the hope of finding the global optimum.[‡] Greedy algorithms are shortsighted in their approach. At each stage of the problem, the greedy rerouting algorithm takes decisions based on information at hand (information about the reroutes already assigned) without worrying about the effect these decisions may have in the future (effects of rerouting other aircraft that have not been considered for rerouting yet). Greedy algorithms produce good solutions for some optimization problems and not for others. For the optimal rerouting problem, the greedy algorithm just pushes the optimality choices over to the aircraft that come later in the sequence of choices and, hence, leads to overall near optimality as explained later in this section.

To understand the working of this algorithm, let us suppose that there are N aircraft affected by the closure of ZFW42 over the period of the optimization horizon. Then, a single rerouting policy consists of a set of N choices, that is, a choice whether to reroute each individual aircraft via the northern route or via the southern route. So, the number of possible rerouting policies is 2^N. An exhaustive search over the entire set of rerouting policies will require 2^N model adaptations to depict the effect of each rerouting policy. Each model adaptation would be followed by model iteration to compute the cost associated with that rerouting policy. In contrast, the greedy search algorithm which would find a possibly optimal rerouting policy by just using $4(N-1)+2$ model adaptations. In general, if there are c reroute choices, this algorithm requires $c^2(N-1)+c$ model adaptations, as opposed to the c^N model adaptations required for an exhaustive search.

We assume that sector ZFW42 is closed down at 05:41:00 UTC on 13 March 2005. The prediction horizon for model adaptations and cost computations associated with a given rerouting policy is a period of 1 h from 05:40:00 to 06:39:00 UTC on 13 March 2005. We chose this time period because this was the time during which we saw the biggest peak in the arrivals from sector ZFW42 to airports within the central ZFW sector, ZFW46. It was seen that during this 1 h period,

[‡]Data available online at http://en.wikipedia.org/wiki/Greedy algorithm [retrieved 1 Feb. 2008].

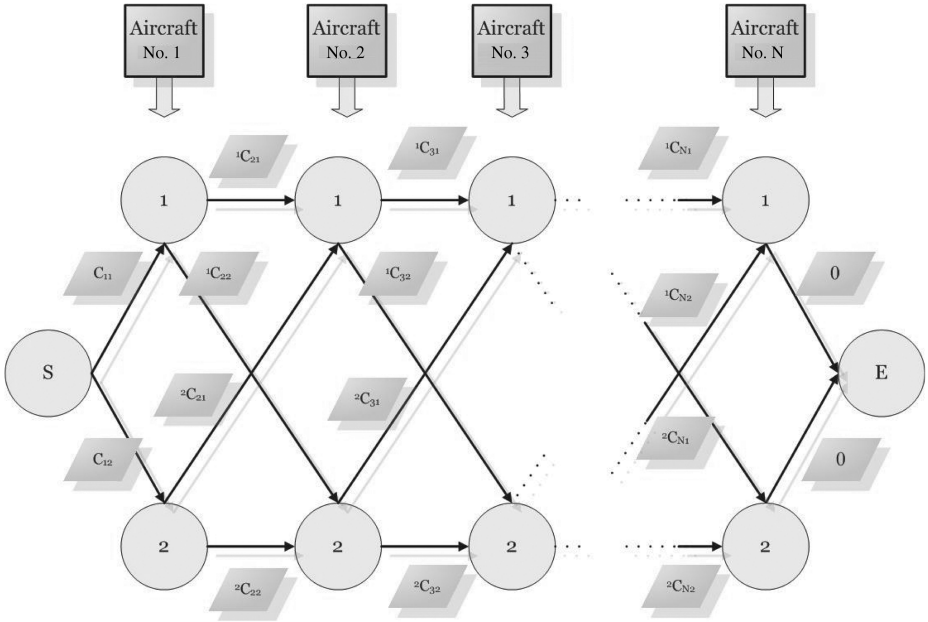

Fig. 7 Network of rerouting decisions.

there were 14 aircraft coming in through sector ZFW42 and landing at airports within ZFW46. The sectors most likely to be overloaded by the resulting rerouting are sector ZFW48, on the northern reroute path, and sector ZFW90, on the southern reroute path. The cost of optimization associated with a particular rerouting policy is set equal to the cumulative number of aircraft by which the Eulerian model predicts that the maximum capacity (25 for sector ZFW48 and 12 for sector ZFW90) of either sector would be violated over the 60 min prediction horizon, if that particular rerouting policy were applied.

$$\text{Cost} = \sum_{k=1}^{N_{\text{horizon}}} \max\{[n(k) - n_c], 0\} \tag{13}$$

where N_{horizon} represents the prediction horizon, $n(k)$ represents the predicted sector count at time step k, and n_c represents the sector capacity.

Figure 7 shows a network of rerouting decisions. Each stage of this network is associated with an individual aircraft. Each node within a given stage represents a route choice for the aircraft. For example, at stage 1, the two nodes represent route choices no. 1 and no. 2 for aircraft no. 1. The algorithm starts from the left-most node S and goes on computing the costs associated with each link in the network as follows: C_{11} is the cost associated with rerouting aircraft no. 1 via route no. 1 (the northern route). This cost is computed as follows: The baseline Eulerian model is adapted to depict aircraft no. 1's changed route. All other affected aircraft are removed from the model during this cost computation. The model is iterated from the start to the end of the prediction horizon, and the sector counts predicted by the model are used to compute the cost C_{11}. Cost C_{12}, the cost associated with rerouting aircraft no. 1 via route no. 2 (the southern route), is computed in a similar manner.

Thereafter, each cost in the network ${}^kC_{ij}$ represents the additional cost associated with rerouting aircraft no. i via route no. j ($j = 1$ or $j = 2$) given that the previous aircraft no. $(i-1)$ has been assigned to route no. k ($k = 1$ or $k = 2$). It is assumed that aircraft no. 1, no. 2, ..., no. $(i-2)$ have been assigned to route choices that are optimal over that partial set given that aircraft no. $(i-1)$ is assigned to route no. k. At stage 2, the cost ${}^1C_{21}$, the additional cost associated with assigning aircraft no. 2 to route no. 1 given that aircraft no. 1 has been assigned to route no. 1, is computed as follows: The baseline Eulerian model is adapted to depict the changed routes of aircraft no. 1 and no. 2. All other affected aircraft are removed from the model during this cost computation. The model is iterated from the start to the end of the prediction horizon, and the sector counts predicted by the model are used to compute the cost associated with this adaptation. Cost C_{11} is subtracted from the resulting cost to obtain ${}^1C_{21}$. Costs ${}^2C_{21}$, ${}^1C_{22}$, and ${}^2C_{22}$ are computed in similar manner. The optimal cost of assigning aircraft no. 2 to reroute no. 1 is computed as follows:

$$C^*_{21} = \min\{(C_{11} + {}^1C_{21}), (C_{12} + {}^2C_{21})\} \tag{14}$$

This cost computation also determines the optimal reroute choice for aircraft no. 1 given that aircraft no. 2 has been assigned to reroute no. 1 (whichever assignment gives the minimum cumulative cost over aircraft no. 1 and no. 2). Cost C^*_{22} and the optimal reroute choice for aircraft no. 1 given that aircraft no. 2 has been assigned to reroute no. 2 are computed in a similar manner.

Then, at stage 3 of the process ${}^1C_{31}$, the additional cost associated with assigning aircraft no. 3 to route no. 1, given that aircraft no. 2 has been assigned to route no. 1, is computed as follows. The Eulerian model is adapted to depict the following changes: aircraft no. 3 is assigned to reroute no. 1; aircraft no. 2 is assigned to reroute no. 1; aircraft no. 1 is assigned to the reroute that was found to be optimal in the computation of C^*_{21}. All other aircraft affected by the closure of ZFW42 are removed from the model. The model is iterated from the start to the end of the prediction horizon, and the sector counts predicted by the model are used to compute the cost associated with this adaptation. Cost C^*_{21} is subtracted from the resulting cost to obtain ${}^1C_{31}$. This process of computing individual link costs followed by partial optimal costs is continued until we reach the right-most node E. At this point, all aircraft have been assigned to their possibly optimal reroute choices, and this is the near optimal rerouting policy.

Greedy algorithms produce good solutions for some optimization problems and not for others. For the rerouting problem, at each stage, the greedy rerouting algorithm makes the routing choice that seems best at that stage. This choice depends on optimization of the cost over a partial set of aircraft, and it may not be optimal when we evaluate the following aircraft. The greedy algorithm never reconsiders the choices that it has made. However, in the case of rerouting, this is a minor drawback because basically, at any given stage of the algorithm, we are penalizing the later aircraft (i.e., aircraft that are yet to be assigned to reroutes) by saying that we have already made choices for the earlier aircraft based on scenarios involving partial sets of aircraft and that the later aircraft will have to be assigned to the less-populated or less-costly reroutes. So, even though we may have incorrectly assigned some of the earlier aircraft to their suboptimal route choices, the later aircraft will be assigned to

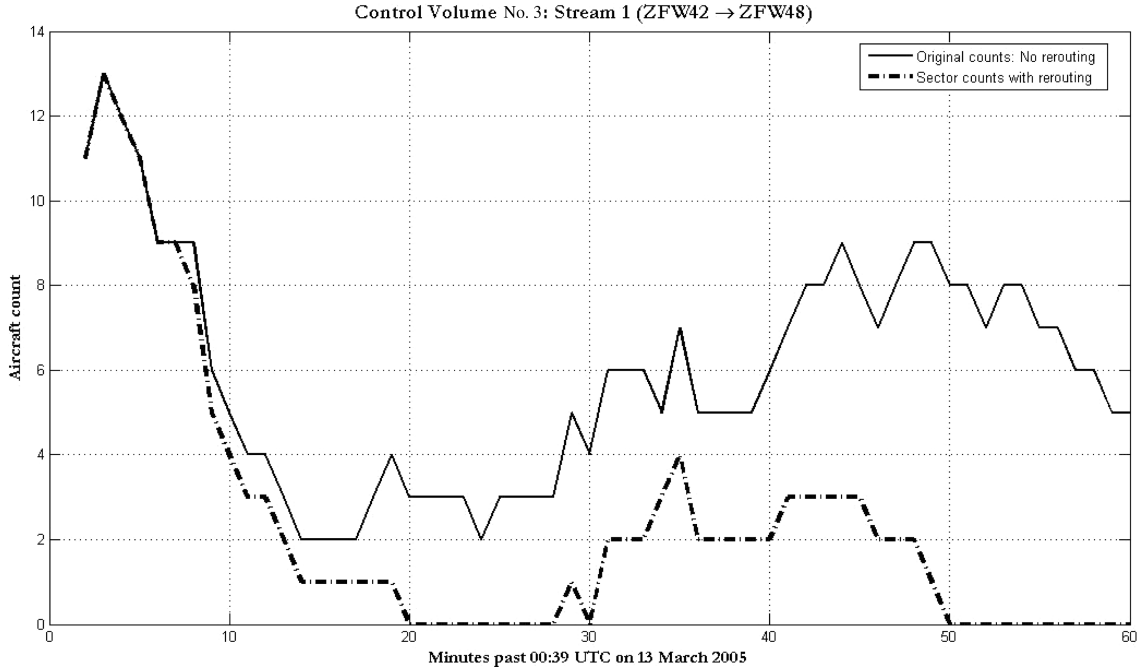

Fig. 8 Comparison of the ZFW42 control volume: stream no. 1 counts with and without rerouting in place.

different reroutes in such a way that we will get overall optimality (or near optimality). Thus, the greedy algorithm just pushes the optimality choices over to the aircraft, which come later in the sequence of choices. We compared the rerouting policy produced by the greedy algorithm with the absolute optimal rerouting policy computed by an exhaustive search, and they agreed with each other in terms of the cost of optimization (i.e., cost associated with the rerouting policy given by the greedy algorithm was equal to the absolute minimum cost).

D. Optimal Rerouting Policy: Results

The greedy search algorithm was applied to the problem of rerouting aircraft around the closed ZFW42 sector. It was found that the optimal policy is to reroute four aircraft via the southern reroute path and the remaining ten affected aircraft via the northern reroute path. Because the Eulerian model indirectly retains trajectory information and identity of individual aircraft, the result also specifies which four aircraft to reroute via the southern reroute path, namely, the first, second, fourth, and fifth aircraft among those aircraft that are supposed to enter sector ZFW42 through the ZME center. So, the optimal rerouting strategy given by the simulation based optimization does not only tell how many aircraft to reroute via a particular alternate route but also specifies which aircraft to reroute via that route.

Figure 8 shows the aircraft counts for stream 1 in sector ZFW42 (this stream consists of aircraft going to sector ZFW48) without rerouting (unbroken line) and the aircraft counts with rerouting in place (dash–dot line). This figure shows that after the sector is closed, all aircraft that were supposed to enter ZFW42 from ZME and then go on to land at airports in ZFW46 are not allowed to enter ZFW42. That is why the dash–dot line is below the unbroken line.

Figures 9 and 10 show stream aircraft counts when all aircraft are rerouted through the northern path (unbroken line), when all aircraft

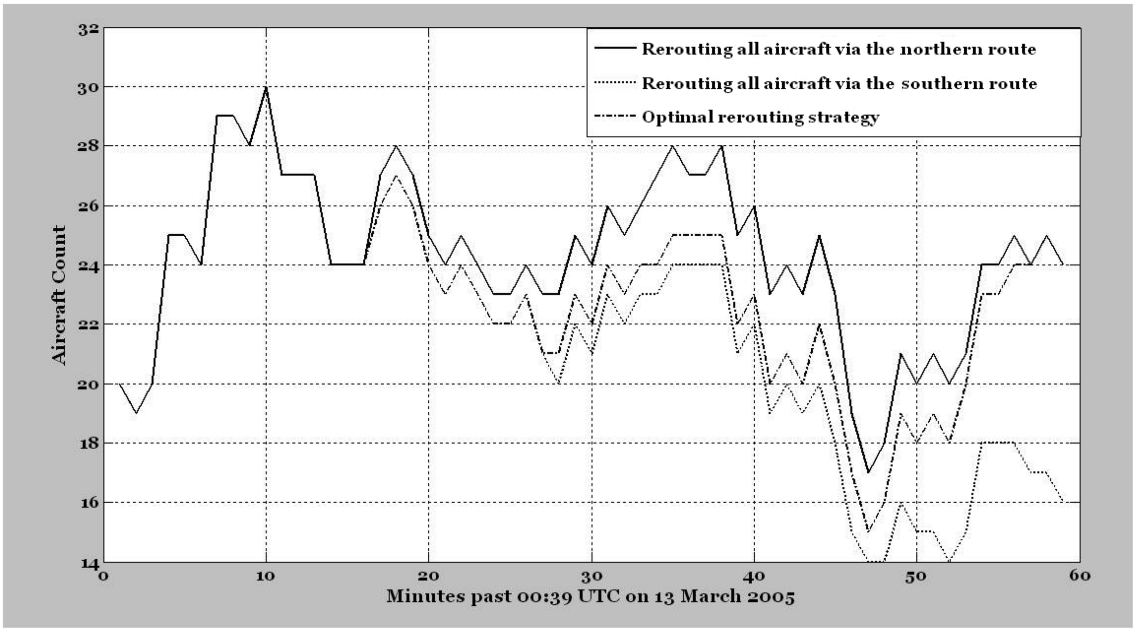

Fig. 9 Comparison of the ZFW48 control volume counts with different rerouting strategies.

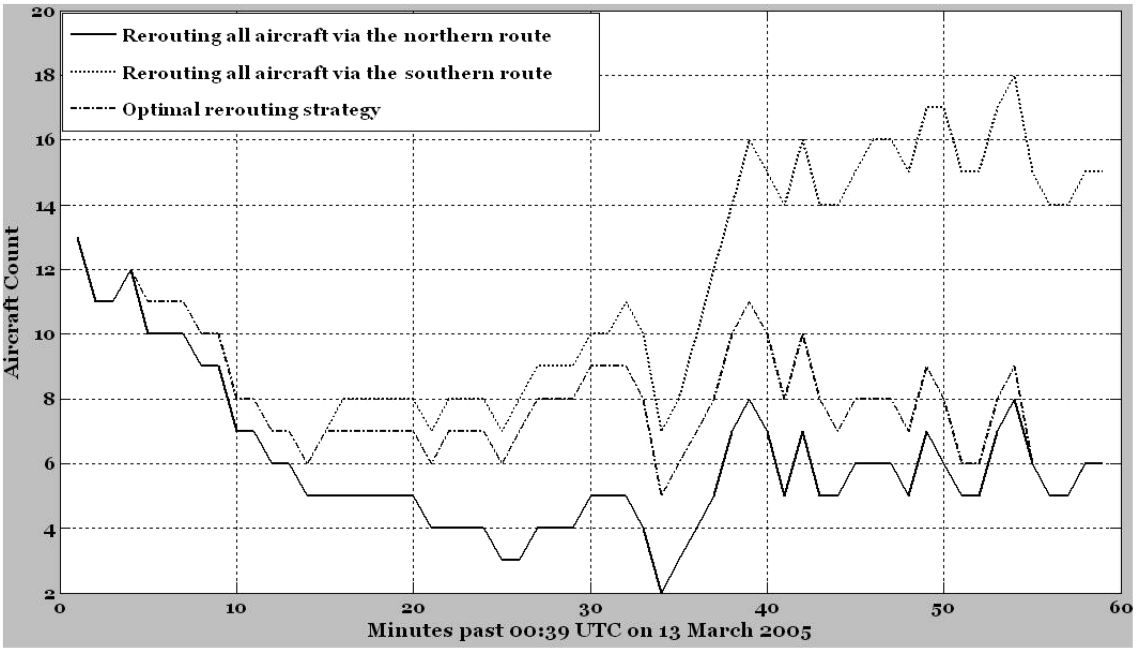

Fig. 10 Comparison of the ZFW90 control volume counts with different rerouting strategies.

are rerouted via the southern path (dotted line), and when the optimal rerouting strategy is applied (dash–dot line). Figure 9 shows aircraft counts for stream no. 3 of ZFW48, and Fig. 10 shows aircraft counts for stream no. 1 of ZFW90 (these two streams consist of aircraft flows going to the central sector, ZFW46, from the respective sectors). As seen from figures, when all the aircraft are rerouted through either one of the alternate routes, the sector along that route gets congested. The optimal rerouting policy keeps the aircraft counts in both the sectors at acceptable levels (below the limit of 25 for sector ZFW48 and the limit of 12 for sector ZFW90, set by the model-based optimization scheme).

V. Conclusions

A new method for online Eulerian airspace model derivation is introduced. This method does not need real-time integration of aircraft trajectories. This method starts with a baseline model, which is derived offline using recorded track data. This baseline model is then adapted, online, to match the real-time traffic situation. As a proof of concept, a baseline model for the Fort Worth center was derived from recorded Enhanced Traffic Management System data for 13 March 2005, for a period of 1 h from 05:00 to 05:59 UTC. This baseline model was validated against the real sector counts observed on that day and time. This model was adapted to match a different traffic situation using information about differences between the two traffic situations. Comparison between the adapted model predictions and real traffic counts showed that the adapted model made perfect aircraft count predictions when the information about the differences between baseline and real time traffic situations was accurate. The main utility of such a low-dimensional model is in fast, online, simulation-based optimization. Application of simulation-based optimization using the adaptive Eulerian model to optimal rerouting decision making is presented.

Results show that the adaptive Eulerian model can be easily and quickly adapted to emulate effects of a variety of air traffic control actions with precision, given accurate information about nominal transit times for each stream within each modeled control volume. In addition to its use in simulation-based optimization schemes, this model will serve as a useful predictive tool for air traffic control personnel. With this adaptive model available to them, they would be able to compare the long-term effects of different candidate traffic flow management actions quickly and to take optimal decisions based on the model predictions. As a continuation of this work, more involved Eulerian models, with different control volumes occupying the same space but containing different aircraft categories, will be investigated. For example, a separate control volume can be used for the relatively slower Very Light Jets (VLJs), whereas the other faster aircraft, like large and heavy jets, could be included in another control volume, although both the control volumes occupy the same physical space. Such a scheme is expected to have some computational advantages. A detailed analysis of differences in transit times for different directions of travel within a given control volume and for different aircraft types is also necessary for increasing the fidelity of the adaptive Eulerian model presented in this paper. In addition, we plan to use this model to speedily compare different strategies for schedule recovery in the presence of convective weather by simulating effects of rerouting aircraft via different routes. Such a comparison tool could be of immense help to the controllers in selecting the best rerouting strategy in bad weather. A faster, intelligent optimization method to search for the optimum set of controls among the finite set of all possible controls (to replace the current method of greedy search) is also a topic for future research.

References

[1] "International Air Transport Association Annual Report," Tech. Rept., *62nd Annual General Meeting of the International Air Transport Association*, International Air Transport Assoc., Montreal, June 2006.

[2] "Global Market Forecast: Future of Flying 2006-25," International Air Transport Assoc. Tech. Rept., http://www.iata.org/events/agm/2005/observers/2005-08-11-agmreport.htm [retrieved 1 Feb. 2008.

[3] Erzberger, H., Davis, T. J., and Green, S. M., "Design of Center-TRACON Automation System," *Proceedings of the AGARD Guidance and Control Panel 56th Symposium on Machine Intelligence in Air Traffic Management*, AGARD, 1993, pp. 11-1–11-12.

[4] Bilimoria, K. D., Sridhar, B., Chatterji, G., Sheth, K. S., and Grabbe, S., "FACET: Future ATM Concepts Evaluation Tool," *Air Traffic Control Quarterly*, Vol. 9, No. 1, 2001, pp. 1–20.

[5] Sridhar, B., Seth, K., and Chatterji, G. B., "Aggregate Flow Model for Air-Traffic Management," *Journal of Guidance, Control, and Dynamics*, Vol. 29, No. 4, July–Aug. 2006, pp. 992–996. doi:10.2514/1.10989

[6] Saraf, A., and Slater, G., "Combined Eulerian Lagrangian Two-Level Control System for Optimal Air Traffic Flow Management," AIAA Paper 2006-6229, Aug. 2006.

[7] Menon, P. K., Sweriduk, G. D., and Bilimoria, K. D., "A New Approach for Modeling, Analysis and Control of Air Traffic Flow," AIAA Paper 2002-5012, Aug. 2002.

[8] Menon, P. K., Sweriduk, G. D., and Bilimoria, K. D., "Air Traffic Modeling, Analysis and Control," AIAA Paper 2003-5712, 2003.
[9] Menon, P. K., Sweriduk, G. D., Lam, T., Diaz, G. M., and Bilimoria, K. D., "Computer Aided Eulerian Air Traffic Flow Modeling and Predictive Control," AIAA Paper 2004-2683, 2004.
[10] Menon, P. K., Sweriduk, G. D., and Bilimoria, K. D., "New Approach for Modeling, Analysis, and Control of Air Traffic Flow," *Journal of Guidance, Control, and Dynamics*, Vol. 27, No. 5, 2004, pp. 737–744. doi:10.2514/1.2556
[11] Bayen, A. M., Raffard, R. L., and Tomlin, C. J., "Eulerian Network Model of Air Traffic Flow in Congested Areas," *Proceedings of the 2004 American Control Conference*, Vol. 6, Inst. of Electrical and Electronics Engineers, New York, 2004, pp. 5520–5526, Catalog No. 04CH37538.
[12] Bayen, A. M., Raffard, R. L., and Tomlin, C. J., "Adjoint Based Constrained Control of Eulerian Transportation Networks: Application to Arrival Traffic Control," *Proceedings of the 2004 American Control Conference*, Vol. 6, Inst. of Electrical and Electronics Engineers, New York, June–July 2004, pp. 5539–5545, ISBN 0-7803-8335-4, INSPEC Accession No. 8434749.